

STEADY STATE SOLUTIONS TO DYNAMICALLY LOADED PERIODIC STRUCTURES

Anthony J. Kalinowski
Naval Underwater Systems Center

SUMMARY

The paper treats the general problem of solving for the steady state (time domain) dynamic response (i.e., NASTRAN rigid format-8) of a general elastic periodic structure subject to a phase difference loading of the type encountered in traveling wave propagation problems. Two types of structural configurations are considered; in the first type, the structure has a repeating pattern over a span that is long enough to be considered, for all practical purposes, as infinite; in the second type, the structure has structural rotational symmetry in the circumferential direction. Due to the periodic nature of the structure and the traveling wave characteristics of the loading, one need only "cut out" and subsequently model a typical periodic region of the total structure, wherein appropriate periodic boundary conditions (i.e., unknown forces and displacements are forced equal, except for unknown phase angle, for corresponding points on both cuts) are used along the cuts. The paper presents both the theory and a corresponding set of DMAP instructions which permits the NASTRAN user to automatically alter the rigid format-8 sequence to solve the intended class of problems. The new input to a standard version NASTRAN run is a set of alter cards, PARAM cards, and direct input matrix (DMI) partitioning arrays which are needed for the purpose of partitioning and correspondingly restructuring the internal NASTRAN mass, damping and stiffness matrices. Final results are recovered as with any ordinary rigid format-8 solution, except that the results are only printed for the typical periodic segment of the structure. A simple demonstration problem having a known exact solution is used to illustrate the implementation of the procedure.

SYMBOLS

[B]	Damping matrix of n^{th} periodic substructure
{ \bar{F} }	Total applied force vector
i	$\sqrt{-1}$
[I ^u]	Diagonal unit identity matrix
I	Number of degrees-of-freedom for interior nodes
[K]	Stiffness matrix of n^{th} periodic substructure

L_p	Spatial period of substructure
L	Number of degrees-of-freedom for left cut nodes
$[M]$	Mass matrix of n^{th} periodic substructure
R	Number of degrees-of-freedom for right cut
t	Time
$\{U\}$	Displacement vector
x	Spatial coordinate
ω	Angular driving frequency
θ, ψ	Angle of incident wave
μ	Phase constant (complex form)
μ^*	Phase constant (real part)

INTRODUCTION

A periodic structure consists of a number of identical substructures, coupled together in identical manners to form the whole system, see for example figure 1a. For such systems, under certain loading conditions, it is often possible to treat only one representative substructure in order to obtain the general response for the whole system. For example, if the loading is exactly the same for all substructures, the latest (and even some earlier) versions of NASTRAN can directly solve this class of problem for both static and steady state cases (i.e., rigid formats 1 and 8). In the case of steady state dynamics problems (rigid format-8) involving traveling wave propagation type inputs, there is a slightly more general loading condition on each periodic substructure, namely that the loading on each substructure is identical except for a known phase constant μ . More specifically, the relation between the applied force vector $\{\bar{F}\}_n$ in the n^{th} substructure and the one, $\{\bar{F}\}_{n+1}$ in the n^{th} substructure is given by

$$\{\bar{F}\}_{n+1} = e^{\mu} \{\bar{F}\}_n \quad (1)$$

where μ is a known phase constant. For the class of problems addressed in this paper, the phase constant is a purely imaginary constant, i.e.,

$$\mu = 0.0 + i\mu^* \quad (2)$$

and physically refers to the fact that there is no difference in energy loss in processing results from one substructure to the next.

Brillouin (ref. 1) points out that wave motion in periodic systems have been studied for nearly 300 years, wherein physicists and electrical engineers have worked in this field in problem areas relating to optics, crystals, electrical transmission liner, etc. (Elachi, ref. 2, provides a comprehensive list of 287 references in this field). Applications of this theory to engineering structural analysis and solid mechanics type problems is only recent. References 3, 4, and 5 are typical of analytical solutions to this type problem for simple configurations consisting of beams, grillages and plate structures. References 6 and 7 represent a significantly more general approach to the problem wherein their application of the theory of finite elements enables one to solve a much larger class of problems involving rather arbitrary structures than one could treat by purely analytical techniques. References 6 and 7 appear to restrict themselves to the problem of determining the conditions (i.e., values of the steady state response frequency ω) under which propagating or non-propagating free wave motion will occur in the absence of explicit external driving forces.

In the work presented here, periodic structures with explicit external driving forces satisfying Equations (1) and (2) are applied to each substructure as illustrated in Figure 1a.

If the loading and spatial boundary conditions on each substructure are the same, except for the phase difference, μ^* , (i.e., the loading for two typical points in two neighboring substructures separated by the period length L_p , are the same except for a multiplying factor of $e^{i\mu^*}$) it follows that the response in each substructure is also the same except for the phase difference μ^* . A simple example of such a case is a propagating pressure wave passing across an infinitely long ribbed plate as illustrated in figure 2b (the plate is in air and no air-structure interaction effects are considered). The propagating surface loading wave is given by the formula

$$p = p_0 e^{i(kx + \omega t)} \quad (3)$$

thus the phase difference between any two neighboring substructures is $\mu^* = kL_p$, where L_p is the spatial period of the periodic system, p_0 is the input loading pressure amplitude, ω is the steady state driving frequency, x is the horizontal spatial coordinate, and k is the wave number of the loading wave.

Other examples of the phase constant relative to a particular example are shown in figure 2. In figure 2a, we have a known pressure wave loading propagating parallel with the axis of the ribbed cylindrical shell; here, the phase constant μ^* is analogous to the figure 2b example and needs no further explanation. In figure 2c, the incident wave is incident at an oblique angle θ and is incorporated into the formula for the phase constant given in the figure 1c.

There is a special case where the ends of the structure do not extend to infinity (i.e., the ends never meet) but instead are connected cyclically, as in figure 3 for example. For such cyclical cases, μ^* must satisfy an additional constraint, namely $\mu^* = 2\pi/n$ where $n = 1, 2, 3, \dots$. For example, in the figure 3 case, $n = 8$, thus $\mu^* = \pi/4$.

We limit ourselves to problems having "one-dimensional periodicity", whereby this term we imply that only two cuts are needed (we shall refer to these as the left and right cuts, see figure 1b) to separate the typical substructure from the system. The response within such a substructure can be, however, multi-dimensional. The remainder of the paper focuses on the procedure for obtaining the displacement and stress response within one typical block of the periodic system. The typical substructure block can be made up of various types of structural elements (including both elements with structural damping and nodes with scalar dampers attached) contained within the NASTRAN library of elements (e.g., CQDMEM, CQDMEM1, CBAR, CONROD ... etc.).

SOLUTION FORMULATION

The solution procedure presented here is very similar to the one in reference (6), except for the fact that here we are considering problems with explicit forcing functions. The first step in the solution procedure is to "cut out" the typical substructure from the overall periodic structure as illustrated in figure 1b and to subsequently replace the cut nodes with the internal forces ($\{\bar{F}_\ell^C\}_n$ for the left cut and $\{\bar{F}_r^C\}_n$ for the right cut) that existed at those nodes before cutting. The displacements at the cut nodes are similarly denoted by $\{\bar{U}_\ell\}_n$ and $\{\bar{U}_r\}_n$ where subscripts ℓ and r denote left and right and the subscript n denotes the n^{th} substructure. Since we are only focusing on the results for the n^{th} substructure, it is convenient to drop the subscript n from here on for notational convenience.

The governing equations of motion for the substructure are first expressed in the familiar finite element form

$$[M]\{\ddot{\bar{U}}\} + [B]\{\dot{\bar{U}}\} + [K]\{\bar{U}\} + \{\bar{F}\} \quad (4)$$

where $[M]$, $[B]$, $[K]$ are the mass, damping and stiffness matrices of the n^{th} substructure respectively; $\{\bar{U}\}$ is the displacement vector of all nodes of the n^{th} substructure; $\{\bar{F}\}$ is the generalized force vector; $(\dot{\quad}) \equiv d(\quad)/dt$, and bars above the variable denote the fact that the variables are complex and that the harmonic time response $e^{i\omega t}$ has not yet been suppressed thus

$$\{\bar{U}\} = \{U\}e^{i\omega t} \quad \{\bar{F}\} = \{F\}e^{i\omega t} \quad (5)$$

The next major step is to partition the matrices and vectors of equation (4) into left cut unknowns, right cut unknowns and interior unknowns (subscripts l, r, i refer to left, right and interior respectively and L, R, I refer to the total number of displacement component unknowns for the left, right and interior domain respectively; note due to periodicity, $L = R$). Thus it follows that after partitioning we have

$$[M] = \begin{bmatrix} M_{ll} & | & M_{li} & | & M_{lr} \\ - & - & | & - & | & - \\ M_{il} & | & M_{ii} & | & M_{ir} \\ - & - & | & - & | & - \\ M_{rl} & | & M_{ri} & | & M_{rr} \\ | & & | & & | \end{bmatrix} \quad (L+R+I) \times (L+R+I)$$

$$[B] = \begin{bmatrix} B_{ll} & | & B_{li} & | & B_{lr} \\ - & - & | & - & | & - \\ B_{il} & | & B_{ii} & | & B_{ir} \\ - & - & | & - & | & - \\ B_{rl} & | & B_{ri} & | & B_{rr} \\ | & & | & & | \end{bmatrix}$$

$$[K] = \begin{bmatrix} K_{ll} & | & K_{li} & | & K_{lr} \\ - & - & | & - & | & - \\ K_{il} & | & K_{ii} & | & K_{ir} \\ - & - & | & - & | & - \\ K_{rl} & | & K_{ri} & | & K_{rr} \\ | & & | & & | \end{bmatrix}$$

$$\{\bar{U}\} = \begin{Bmatrix} \bar{U}_l \\ \text{---} \\ \bar{U}_i \\ \text{---} \\ \bar{U}_r \end{Bmatrix} \quad (6)$$

$$(1) \times (L+R+I)$$

$$\{\bar{F}\} = \begin{Bmatrix} \bar{F}_l^c \\ \text{---} \\ 0 \\ \text{---} \\ \bar{F}_r^c \end{Bmatrix} + \begin{Bmatrix} \bar{F}_l^a \\ \text{---} \\ \bar{F}_i^a \\ \text{---} \\ \bar{F}_r^a \end{Bmatrix}$$

Note the generalized force vectors $\{\bar{F}\}$ has been further decomposed as the sum of an unknown force vector, $\{\bar{F}^c\}$, (which denotes the yet unknown internal forces existing at the cuts in the structure) and a known applied force vector, $\{\bar{F}^a\}$, (which denotes all known forces existing within and at the cuts of the periodic substructure).

The full periodic structure is cut (left and right cuts), therefore it follows that the internal nodal forces normally existing at the cuts now play the role of external (as yet unknown) applied forces.

The special case of an externally applied force appearing at a left or right cut requires special attention in that one component of the total force vector is due to the externally applied force and the other component is due to the internal force at the cut. The external force value on a cut must be shared between the generic substructure block being analyzed and its immediate neighbor; consequently these end type external force values are divided in half (see, for example, the situation in figure 1c where node 1 lies on the left cut).

A further relation that is needed in the formulation relates to the fact that the right end of the n^{th} generic substructure is the beginning (left end) of the $n+1$ generic substructure, thus from Equation (1) it follows that

$$\begin{aligned} \{\bar{F}_r^C\} &= -e^{\mu} \{\bar{F}_\ell^C\} \\ \{\bar{U}_r\} &= e^{\mu} \{\bar{U}_\ell\} \end{aligned} \tag{7}$$

where the minus sign in the first of Equation (7) accounts for the fact that internal nodal forces acting as external forces on the right cut of generic substructure n are opposite in sign to the internal nodal forces acting on the left cut neighboring substructure $n + 1$.

The next step in the development is to substitute Equations (5) and (6) into Equation (4); the subsequent cancellation of $e^{i\omega t}$ permits us to drop the bar superscript notation thus arriving at a "reduced form of Equation (4)". At this point there are five groups of unknowns, namely $\{U_r\}$, $\{U_\ell\}$, $\{U_i\}$, $\{F_r^C\}$, $\{F_\ell^C\}$. The three row partitions of the reduced Equation (4) in conjunction with the two Equations (7), provide $3 + 2 = 5$ corresponding groups of equations to balance the five groups of unknowns. Next, we substitute Equations (7) into the reduced form of Equation (4), and subsequently employ the third row partition of reduced Equation (4) to eliminate the $\{F_\ell^C\}$ unknown. Doing these operations result in the following set simultaneous equations for the displacement unknowns $\{U_\ell\}$ and $\{U_i\}$:

$$\begin{bmatrix}
-\omega^2 [MLL] + & | & -\omega^2 [MLI] + \\
i\omega [BLL] + & | & i\omega [BLI] + \\
[KLL] & | & [KLI] \\
\hline
-\omega^2 [MIL] + & | & -\omega^2 [MII] + \\
i\omega [BIL] + & | & i\omega [BII] + \\
[KIL] & | & [KII]
\end{bmatrix} \cdot \begin{Bmatrix} \{U\}_\ell \\ \vdots \\ \{U\}_i \end{Bmatrix} = \begin{Bmatrix} \{F_\ell^a\} + e^{-\mu \cdot i} \{F_r^a\} \\ \vdots \\ \{F_i^a\} \end{Bmatrix} \quad (8)$$

(L+I) x (L+I) matrix
(1) x (L+I) vector

where

$$\begin{aligned}
[MLL] &= [M_{\ell\ell}] + \text{Cos}\mu^* [M_{\ell r}] + \text{Cos}\mu^* [M_{r\ell}] + [M_{rr}] \\
[BLL] &= [B_{\ell\ell}] + \text{Cos}\mu^* [B_{\ell r}] - \omega \text{Sin}\mu^* [M_{\ell r}] + (\text{Sin}\mu^*/\omega) [K_{\ell r}] \\
&\quad + \text{Cos}\mu^* [B_{r\ell}] + [B_{rr}] + \omega \text{Sin}\mu^* [M_{r\ell}] - (\text{Sin}\mu^*/\omega) [K_{r\ell}] \\
[KLL] &= [K_{\ell\ell}] + \text{Cos}\mu^* [K_{\ell r}] - \omega \text{Sin}\mu^* [B_{\ell r}] \\
&\quad + \text{Cos}\mu^* [K_{r\ell}] + [K_{rr}] + \omega \text{Sin}\mu^* [B_{r\ell}] \\
[MLI] &= [M_{\ell i}] + \text{Cos}\mu^* [M_{r i}] \\
[BLI] &= [B_{\ell i}] + \text{Cos}\mu^* [B_{r i}] + \omega \text{Sin}\mu^* [M_{r i}] - (\text{Sin}\mu^*/\omega) [K_{r i}] \\
[KLI] &= [K_{\ell i}] + \text{Cos}\mu^* [K_{r i}] + \omega \text{Sin}\mu^* [B_{r i}] \\
[MIL] &= [M_{i\ell}] + \text{Cos}\mu^* [M_{i r}] \\
[BIL] &= [B_{i\ell}] + \text{Cos}\mu^* [B_{i r}] - \omega \text{Sin}\mu^* [M_{i r}] + (\text{Sin}\mu^*/\omega) [K_{i r}] \\
[KIL] &= [K_{i\ell}] + \text{Cos}\mu^* [K_{i r}] - \omega \text{Sin}\mu^* [B_{i r}] \\
[MII] &= [M_{ii}] \\
[BII] &= [B_{ii}] \\
[KII] &= [K_{ii}]
\end{aligned} \quad (9)$$

At this point, the linear set of complex algebraic Equations (8) can be solved for the unknown displacements $\{U_\ell\}$, $\{U_i\}$. The unknown displacement at the right cut, $\{U_r\}$ can be easily computed with the second of equation (7). The

size of the algebraic system is governed by the $(L+I) \times (L+I)$ coefficient matrix (i.e., matrix multiplying the unknown displacement vector) where $L+I$ equals the number of left cut, L , plus interior, I , unknown displacement components. Typically $I \gg L$, therefore it is not a very big additional burden on the equation solver to include the second of Equation (7) as part of the overall system (actually, we add R extra unknowns, $\{U_r\}$, and R extra equations (where R = number of right cut unknowns). Thus in place of Equation (8), we consider the slightly larger, but equivalent system of

$$\begin{bmatrix}
 -\omega^2 [MLL] + & -\omega^2 [MLI] + & \\
 i\omega [BLL] + & i\omega [BLI] + & [0] \\
 [KLL] & [KLI] & \\
 \text{---} & \text{---} & \text{---} \\
 -\omega^2 [MIL] + & -\omega^2 [MII] + & \\
 i\omega [BIL] + & i\omega [BII] + & [0] \\
 [KIL] & [KII] & \\
 \text{---} & \text{---} & \text{---} \\
 i\omega [BRL] + & & \\
 [KRL] & [0] & [KRR]
 \end{bmatrix} \cdot \begin{Bmatrix} \{U_l\} \\ \\ \\ \\ \\ \\ \\ \{U_r\} \end{Bmatrix} = \begin{Bmatrix} \{F_l^a\} + \\ e^{-\mu \cdot i} \{F_r^a\} \\ \text{---} \\ \{F_i^a\} \\ \text{---} \\ \{0\} \end{Bmatrix} \quad (10)$$

$(L+I+R) \times (L+I+R)$
 coefficient matrix

where

$$\begin{aligned}
 [BRL] &= (\sin \mu^* / \omega) [I^u] \\
 [KRL] &= \cos \mu^* [I^u] \\
 [KRR] &= -[I^u]
 \end{aligned} \quad (11)$$

and $[I^u] \equiv$ diagonal unit identity matrix

The RI block of the displacement coefficient matrix in Equation (10) above is identically zero, thus the bottom R rows of the system of simultaneous equations are totally independent of the solution to the top $L+I$ rows. The length of the solution vector $L+I+R$ is of exactly the same length of the original substructure matrix (Equations (4) and (6)), consequently the modification of the DMAP instructions becomes simpler because of the fact that one need only intercept the logic of the equation solver and replace the existing mass stiffness and damping matrices with the modified matrices defined by the new coefficient matrix of Equation (10) (and associated new entry definitions from Equations (9) and (11)). Since the length of the solution vector is still the same

as the original problem before modification, the post processing DMAP operations for displacement printout, stress recovery, etc. need not be modified.

An alternate scheme (although not yet implemented) would be to modify the input to the complex equation solver to accept the smaller $(L+I) \times (L+I)$ coefficient matrix used in Equation (8) directly. After solving the smaller $L+I$ length displacement vector, the full vector (i.e., attaching the missing $\{U_r\}$ portion) can be formed by expanding it to length $L+I+R$ via the second of Equation (7). Finally, stress and displacement results can be processed in the usual way with existing DMAP operations.

RIGID FORMAT-8 DMAP MODIFICATION FOR NASTRAN

The periodic structure capability described in the previous section can be implemented in a standard version of NASTRAN. In particular, the DMAP sequence required to perform the necessary operations are listed in Appendix A. This DMAP sequence was checked out on an 1108 computer, standard version of level 15.5 NASTRAN and is introduced in the EXECUTIVE CONTROL deck with the following instructions:

ALTER 138

(see Appendix A for specific instructions)

ALTER 139,139

(replace KDD, BDD, MDD with KDDX, BDDX, MDDX
within call arguments of FFRD module
see Appendix A for detailed instruction)

level 15.5
implementation

ALTER 140

(Conditional print statement, see Appendix-
A for detailed DMAP instructions)

These same level 15.5 DMAP instructions can also be applied to level 17.0 NASTRAN, the only difference being that

replace ALTER 138 with ALTER 158

replace ALTER 139,139 with ALTER 159,159

replace ALTER 140 with ALTER 160

It is pointed out, however, that the level 17.0 modifications described above have not actually been tried although due to the similarity of the change, the DMAP sequence is expected to work.

It is important to note that we are modifying the standard NASTRAN unknown displacement vector coefficient matrix just prior to the entry into the FFRD module used for the solution to the simultaneous complex algebraic equations. The implication of this statement is that the row numbering scheme for the displacement vector has already accounted for the fact that single point constraints, multipoint constraints and omitted coordinates have already been accounted for. Thus, for example, the length of the $\{U_\ell\}$ vector, L, is not simply the number of nodes on the left cut times the degrees-of-freedom per node, but rather is less by the amount corresponding to the number of SPC's, MPC's and OMIT's relating to the nodes along the left cut. Similar comments apply to the length of the $\{U_i\}$ and $\{U_r\}$ vectors. The understanding of the above displacement vector length comments must be clearly understood by the user before attempting to fill out the input data matrix partitioning vectors CV100, CV010, CVO01 defined later in this paper.

INPUT DATA FOR NASTRAN RUN

The BULK DATA input to a typical periodic structure run consist of two basic parts. The first part corresponds to the usual bulk data input cards normally required to make a NASTRAN run (e.g., GRID CARDS, ELEMENT CARDS, DAREA CARDS, FREQ CARD, DLOAD CARD, etc.); the second part consists of special input cards that are explained in the following text.

PARAM Cards

These cards are used to enter various matrix coefficients appearing in Equations (9) and (11); especially the constants

<u>Text Variable</u>	<u>Computer Variable</u>	
$\text{Cos}\mu^*$	\equiv CMST	
$0.0 + i\omega$	\equiv FI MEG	
$-\omega^2$	\equiv N MEG2	
-1.0	\equiv N NE	
$-\sin\mu^*/\omega$	\equiv NSMSB Ø	(12)
$-(\sin\mu^*)\omega$	\equiv NSMST Ø	
+1.0	\equiv P NE	
$\sin\mu^*/\omega$	\equiv SMSB Ø	note: 0 = zero
$(\sin\mu^*)\omega$	\equiv SMST Ø	Ø = letter

are read in on standard NASTRAN PARAM cards where μ^* is the phase angle defined in Equation (2) and ω is the angular driving frequency in radians per second ($\omega = f \cdot 2\pi$ where f = driving frequency in Hz specified on the FREQ card). The format for a typical PARAM card is:

Col's 1 - 8	PARAM
Col's 9 - 16	one of the 8 computer variable names defined by Equation (12)
Col's 17 - 24	real part of variable defined in Col's 9-16
Col's 25 - 32	imaginary part of variable defined in Col's 9-16 (only non zero entry is for variable FIØMEG)

Comments

Strictly speaking, the real part of variable FIØMEG should be 0.0; however, for the NUSC Univac 1108, operating with the level 15.5 version of NASTRAN used to implement the procedure, an arbitrary small number is entered (say 1.0×10^{-20}) in order to avoid a strange system type error message that is printed when exactly 0.0 is entered as the real part. The FIØMEG variable is only used to compute and subsequently print out the internal forces at the cuts after all the main calculations for displacement are completed. The mentioned error message probably will not appear if other NASTRAN versions and/or other computer systems are used.

DMI Cards for Matrix Partitioning

A set of DMI direct matrix input cards are needed to provide the information NASTRAN needs to partition the mass, damping and stiffness matrices. Three groups of cards are needed; a column partitioning vector for the left cut group of displacement node components, CV100; a column partitioning vector for the interior group of displacement node components, CV010; and a column partitioning vector for the right cut group of displacement node components, CV001. A set of row partitioning vectors are automatically generated by the Appendix A DMAP instructions. The column partitioning are made up of entries that are either 1.0 or 0.0. Since all entries within NASTRAN are assumed to be zero unless otherwise specified, the user need only enter 1.0 values in the appropriate slot in each of the above mentioned partitioning vectors. The rules are simple and are as follows:

- Formation of left cut partitioning vector CV100

Enter a 1.0 in each row number corresponding to each active independent component degrees-of-freedom lying along the left cut. The length of the CV100 vector is $L+I+R$ and there should be L 1.0 entries (the remaining $I+R$ entries are automatically zero by virtue of not

being defined). If the left cut nodal numbering pattern is sequential and starts with the lowest node number of the whole system (e.g., node 1, 2, 3, . . .), then the first L entries of CV100 will be all 1.0 values. However, if the left cut numbering scheme does not contain only the lowest node numbers, but instead the whole system is numbered at random, then the L 1.0 entries will correspondingly be distributed throughout the CV100 vector, and the "bookkeeping" involved with defining the CV100 vector becomes messy. The user having MPC's, SPC's or OMIT's applied to nodes along the left cut must be sure to account for these during the process of entering the 1.0 values into the partitioning vector CV100.

- Formation of the interior partitioning vector CV010

Enter a 1.0 in each row number corresponding to each active independent component degree-of-freedom lying on the interior of the structure. The length of the CV010 vector is $L+I+R$ and there should be I 1.0 entries (the remaining $L+R$ entries are automatically zero). If the interior nodes are numbered sequentially, (following the same sequential pattern used in the CV100 vector), then the middle $L+1$, $L+2$, . . . $L+I$ entries of the CV010 vector will all be 1.0 values. Again remember to account for SPC's, MPC's and OMIT's in the numbering scheme.

- Formation of the right cut partitioning vector CV001

Enter a 1.0 in each row number corresponding to each active independent component degree-of-freedom lying on the right cut of the periodic structure. The length of the CV001 vector is $L+I+R$ and there should be R 1.0 entries (the remaining $L+I$ entries are automatically zero). If the left cut, interior, and right cut nodes are all numbered sequentially (in the respective order mentioned), then the ending $L+I+1$, $L+I+2$, . . . $L+I+R$ entries of the CV001 vector will all be 1.0 values. Again remember to account for SPC's, MPC's and OMIT's in the numbering scheme.

DMI Cards Format

The bulk data cards for the definitions of the partitioning vectors via the standard DMI cards is as follows:

- CV100 vector cards

<u>Col's</u>	<u>Entry</u>
	first header card
1-8	DMI
9-16	CV001
17-24	0

<u>Col's</u>	<u>Entry</u>
25-32	2
33-40	1
41-48	1
49-56	blank
57-64	integer value equal to magnitude of (L+R+I)
65-72	1
	second card
1-8	DMI
9-16	CV001
17-24	1
25-32	enter integer row number ,say N1, of first 1.0 entry
33-40	1.0 for entry N1
41-48	1.0 or 0.0 for entry N1+1
49-56	1.0 or 0.0 for entry N1+2
57-64	1.0 or 0.0 for entry N1+3
65-72	1.0 or 0.0 for entry N1+4
73-80	Continuation card name, say CONT1, if needed.
	third continuation card (if needed)
1-8	+ONT1
9-16	1.0 or 0.0 for entry N1+ 5
17-24	. .
25-32	. .
33-40	. .
41-48	. .
49-56	. .
57-64	. .
65-72	1.0 or 0.0 for entry N1+12
73-80	Continuation card name, say CONT2, if needed.
	fourth continuation card (if needed)
	similar to third continuation card ... etc.

- CV010 Vector Cards

These cards are made up analogously to the CV100 vector already described above, the only differences being that on the first two cards, replace CV100 with CV010; also, the number of the first 1.0 entry slot (N1 value in col's 25-32 of the second CV100 data card) is different.

- CV001 Vector Cards

These cards are made up analogously to the CV100 vector already described above, the only differences being that on the first two cards, replace CV100 with CV001; also the number of the first 1.0 entry slot (N1 value in col's 25-32 of the second CV100 data card) is different.

Finally, examples of making the partitioning cards is given later in a demonstration problem.

DMI Cards for Merge Operations

A set of DMI direct matrix input cards are needed to define certain dummy matrices which NASTRAN needs to successfully merge certain internal matrices within the Appendix-A DMAP sequence. These input cards will consist of a group of eight cards that must always be included for a run. The only thing that changes from one NASTRAN run to another is the lengths of these dummy arrays. These dummy null arrays are only introduced to avoid DMAP error message printouts for Univac 1108, level 15.5 NASTRAN that occurred when the lead matrix entry in the standard DMAP MERGE operation is not defined.

DMI Cards Format

<u>Col's</u>	<u>Entry</u>
	first header card
1-8	DMI
9-16	LIXLI enter characters, (does not mean multiply LI times LI)
17-24	0
25-32	2
33-40	1
41-48	1
49-56	blank
57-64	enter integer equal to L plus I
65-72	enter integer equal to L plus I
	second card
1-8	DMI
9-16	LIXLI
17-24	1
25-32	1
33-40	0.0
	third card
	same as first card, except
Col's 9-16	enter LIXL2
Col's 57-64	enter integer equal to L plus I
Col's 65-72	enter integer equal to L plus L
	fourth card
	same as second card, except
Col's 9-16	enter LIXL2

fifth card
 same as first card, except

Col's 9-16 enter L2XLI
 Col's 57-64 enter integer equal to L plus L
 Col's 65-72 enter integer equal to L plus I

sixth card
 same as second card, except

Col's 9-16 enter L2XLI

seventh card
 same as first card, except

Col's 9-16 enter L2XL2
 Col's 57-64 enter integer equal to L plus L
 Col's 65-72 enter integer equal to L plus L

eighth card
 same as second card, except

Col's 9-16 enter L2XL2

DMI Cards for Unit Matrix Definition

Finally, a set of DMI direct matrix input cards as needed to define the unit matrix $[I^u]$ employed in Equation (11).

DMI Cards Format

<u>Col's</u>	<u>Entry</u>
	first header card
1-8	DMI
9-16	UMATR
17-24	0
25-32	6
33-40	1
41-48	2
49-56	blank
57-64	enter integer equal to L plus L
64-72	enter integer equal to L plus L

<u>Col's</u>	<u>Entry</u>
	second card
1-8	DMI
9-16	UMATR
17-24	1
25-32	1
33-40	1.0
	third card
	same as second card, except
Col's 17-24	enter 2
Col's 25-32	enter 2
	fourth card
	same as second card, except
Col's 17-24	enter 3
Col's 25-32	enter 3
	.
	.
	etc.
	.
	.
	last (L+1 st) card
	same as second card, except
Col's 17-24	enter integer value equal to L
Col's 25-32	enter integer value equal to L

DEMONSTRATION PROBLEM

The use of the DMAP sequence in conjunction with the new PARAM and DMI input cards defined in the previous section will perhaps be better understood by including a specific example solution that has the features that (1) is a small size problem convenient for matrix operation checking and debugging purposes; (2) contains most of the main ingredients typical of a representative problem, thus the system has mass, stiffness, and damping; (3) the exact solution to the problem is known for checking purposes. The problem illustrated in figure 4a meets all of these conditions, and corresponds to a plane pressure wave propagating in an infinite acoustic fluid medium. Upon sampling the pressure response along any two parallel vertical cuts (separated by the horizontal distance L_p) it can be shown that the response (pressure and displacement) is different only by the amount $e^{i\mu^*}$ where for this particular problem

$$\mu^* = \left(\frac{\omega}{c}\right)(L_p) \cos\psi \quad (13)$$

where ω = driving frequency (rad/sec), L_p = length (in.) between two parallel cuts, c = compressional wave speed (in/sec); ψ = angle of incident wave. The solution for the pressure and motion response is sought for the shaded region shown in figure 4a. Only the dotted outlined region is modeled with finite elements and is correspondingly shown in figure 4b.

In order to exercise this demonstration problem to the fullest extent, we will use different types of boundary conditions on all four sides of the figure 4b finite element model.

Boundary Conditions

- Left and right vertical cuts

Since this problem falls within the class of problems solvable by the phase difference type boundary condition, boundary conditions specified by Equations (7) are enforced. Here the left and right cut forces and displacements are taken as unknowns.

- Top face

The boundary condition for the top face is different from the left and right face in that here we explicitly apply the free field pressure (converted into equivalent nodal forces). The formula for the freely propagating pressure wave is given by the expression

$$\bar{p}(x,y,t) = \underbrace{p_0 e^{i(kr)}}_{p(x,y)} e^{i\omega t} \quad (14)$$

where $k = \omega/c = \text{wave number (in.}^{-1}\text{)}$

$r = \text{spatial coordinate normal to direction of wave propagation (in.)}$

$p_0 = \text{steady state pressure amplitude (psi)}$

$$i = \sqrt{-1}$$

$p = \text{pressure (psi) (spatial variation)}$

and r is related to the x,y coordinates by the relation

$$r = x \cos\psi + y \sin\psi \quad (15)$$

The y -direction force at upper face node 3 is computed by substituting $p(x,H)$ from Equation (14) into the expression

$$\left({}_3F_{\ell y}^a \right) = \int_{x=0}^{x=L_p/4} -p(x,H) dx \quad (16)$$

the force at upper face node 4 is computed similarly by

$$({}_4F_i^a)_y = \int_{x=L_p/4}^{x=3L_p/4} -p(x,H)dx \quad (17)$$

and finally the upper face node 9 is computed similarly by

$$({}_9F_r^a)_y = \int_{x=3L_p/4}^{x=L_p} -p(x,H)dx \quad (18)$$

The demonstration problem is evaluated for the following specific input data:

$$\begin{aligned} p_0 &= 100. \text{ psi} \\ c &= 60000. \text{ in/sec} \\ L_p &= 2.0 \text{ in.} \\ H &= 2.0 \text{ in.} \\ f &= \omega/2\pi = 3000. \text{ Hz} \\ \psi &= 45^\circ \\ p &= \text{mass density} = .000096 \text{ lb.-sec/in}^4 \end{aligned} \quad (19)$$

Substituting the above Equation (19) input constant into Equations (16), (17) and (18) results in

$$\begin{aligned} ({}_3F_\ell^a)_y &= -49.8972 e^{i 28.6378^\circ} \\ ({}_4F_i^a)_y &= -99.7944 e^{i 38.1837^\circ} \\ ({}_9F_r^a)_y &= -49.9742 e^{i 47.7297^\circ} \end{aligned} \quad (20)$$

An important point must be made regarding loading the final force array $\{\bar{F}\}$ (Equation (4)) for the periodic structure problem. Observation of the Equation (10) loading vector of the new periodic structure problem statement, reveals that the left cut applied forces, $\{F_\ell^a\}$, are applied, as normal, to the corresponding left cut node; also, the interior applied forces, $\{F_i^a\}$, are applied, as normal, to the corresponding interior nodes; however, the right

cut applied forces, $\{F_r^a\}$, are not applied to the right cut nodes, but rather, are first multiplied by the complex constant $e^{-\mu^*i}$, and then applied to the corresponding left cut node. For the demonstration problem at hand, substituting Equation (19) into Equation (13) implies that $\mu^* = 25.45584^0$, thus

$$e^{i\mu^*} ({}_yF_r^a) = -49.9742 e^{i22.27387^0} \quad (21)$$

therefore, in summary, at node number 3 in the y direction apply a net sum

$$\text{force} = -49.8972 e^{i28.6378^0} -49.9742 e^{i22.27387^0} \quad (22)$$

and at node number 4 in the y direction apply a net

$$\text{force} = -99.7944 e^{i38.1837^0} \quad (23)$$

and at node number 9 in the y direction apply a net

$$\text{force} = 0.0 \text{ (i.e., do not apply any force).}$$

- Bottom face

The boundary condition for the bottom face could have been selected similar to the top face (i.e., we convert the pressure into equivalent nodal forces). However, instead we use a slightly more complicated boundary condition that permits us to introduce a [B] matrix entry into the problem. More specifically, the pressure and normal velocity along the bottom cut can be obtained from the expression

$$p(x,0) = \rho c V_n \quad (24)$$

where V_n is the particle velocity normal to the wavefront propagation direction. Therefore the relation between the V_y velocity component and the y direction resisting reaction is given by

$$({}_yF_i^a) \approx (p(x,0) \cdot \Delta A) = \underbrace{\rho c \Delta A \text{ Sin} \psi}_{\text{damping constant} \equiv C_d} V_y \quad (25)$$

Thus, the bottom face boundary condition (simulating an approximate wave absorbing boundary condition) is achieved by placing viscous dampers along the bottom cut (see figure 4b), wherein the damper constants are defined by

$$C_d = \rho c \Delta A \text{ Sin} \psi \quad (26)$$

where ΔA is an appropriate area factor relating the pressure and concentrated force $({}_yF_i^a)$. When the wave length of the incident wave is long relative to

the mesh size, one can set $\Delta A =$ the surface element length for bottom surface nodes off the cuts and set $\Delta A = 1/2$ the surface element length for the nodes lying on the cuts. Thus for the demonstration problem at hand, $C_d = 8.14587$ for the middle damper and half that amount for the end cut dampers.

Preparation of Demo NASTRAN Input Data

- executive control

The form of the DMAP instructions presented in Appendix A are general and are not problem dependent. The only times the user deviates from the presented DMAP sequence is (1) when he switches from one level of NASTRAN to another wherein the ALTER statement numbers change; or (2) when he wishes to turn off or turn on the intermediate matrix printout switch ISW, defined in the third DMAP ALTER statement (ISW = +1 prints all intermediate matrix operation steps in addition to a printout of the FORVEC vector which lists the left cut, interior, and right cut nodal forces; ISW = -1 no intermediate printout).

- case control

The standard CASE CONTROL deck is shown in the APPENDIX A, wherein the only thing worth noting is the fact that a DLOAD card is used for the purpose of superimposing the two vectors $\{F_\ell^a\}$ and $e^{-\mu^*i} \{F_r^a\}$ which are both applied to the same left cut nodes (in correspondence with the first partition of Equation (10)).

- bulk data

The CDAMP2 cards are used to define the damping constants applied at the bottom surface nodes. The CQDMEM membrane elements (and corresponding MAT2, PQDMEM cards) are used to define the fluid media, employing the displacement fluid element approach described in ref. 8. The collection of DLOAD, DAREA, DPHASE, RLOAD1, TABLED1 cards are used to insert the applied forces defined by Equations (22) and (23). The GRDSET card is employed to eliminate the non-applicable 3, 4, 5, 6 degrees-of-freedom for the 2-D membrane elements. Standard GRID cards define node coordinates and the standard FREQ card defines frequency of $f = \omega/2\pi = 3000$ Hz. The special nine PARAM cards defined by Equations (12) are evaluated using the data in Equations (19). In the case of the DMI cards for the partitioning vectors CV100, CV010, CV001, the first thing to establish for the problem is the sizes L, R, I for the individual partitions. It is convenient, for bookkeeping purposes, to number the left cut sequentially; and to also number the interior sequentially (with the lowest interior node number appearing next to the highest left cut node number) and finally number the right cut sequentially with the lowest right cut node appearing next

to the highest internal node number. Thus for the problem at hand[†], $L = 2$ degrees-of-freedom/node times 3 left cut nodes = 6; $I = 2$ degrees-of-freedom/node times 3 interior nodes = 6; and $R \equiv L = 6$ due to the periodicity of the structure. The first 6 entries of CV100 are 1.0, the rest of the entries are zero; the 7th through 12th entries of CV010 are 1.0, the rest being zero; and finally the 13th through 18th entries of CV001 are 1.0, all other entries being zero. The 8 merging DMI cards LIXLI...L2XL2 are defined according to the instructions given earlier in the paper and need no further comment. Finally the unit matrix DMI cards for the UMATR matrix are defined according to the instructions given earlier in the paper.

Results of NASTRAN Demo Problem

Selected output results for the figure 4b demonstration problem are presented as NASTRAN direct printout (real and imaginary part type output format) in APPENDIX B. The first part of the NASTRAN printout illustrates the net input vector (e.g., results of Equations (22) and (23)); it is always good to include as a checking feature of the input.

Next the stress output is printed and refers to the stress computed at the center of the element. Note that due to the sign convention difference regarding stress and pressure (opposite in sign, see ref. 8 for details), the user must reverse the sign of stress to obtain the pressure, i.e.,

$$p = -\sigma_{xx} = -\sigma_{yy}$$

It should be noted that the NASTRAN output format headings are in error (due to a formatting bug in NASTRAN that has remained in practically all levels of NASTRAN); the output heading should be read as follows (for each element row of stress output): Real Pt. (σ_{xx}), Real Pt. (σ_{yy}), Real Pt. (σ_{xy}), Img. Pt. (σ_{xx}), Img. Pt. (σ_{yy}), Img. Pt. (σ_{xy}). The results shown in APPENDIX B, Table B-1, show the NASTRAN results next to the exact solution, after converting the real and imaginary parts into amplitude and phase data.

The exact solution is evaluated with $p(x,y)$ from Equation (14) at distances r that locate a line (drawn parallel to the wave front) which passes through the midpoint of an element. The NASTRAN results agree quite well with the exact solution in both phase and amplitude. It is noted that a very slight asymmetry exists between the NASTRAN phase angle results for element 3 and element 4. This is probably due to the fact that the boundary conditions on the top and right cut surfaces do not result in exactly the same applied nodal forces (e.g., the top forces were not computed using a consistent pressure-to-force application formula that involves the displacement shape functions). A similar comment applies to the relation between the bottom surface forces and left cut

[†]Suppose, for illustrative purposes, node 5 had the x displacement SPC constrained to zero and suppose the x displacement of node 4 was forced (through an MPC relation) to equal the x displacement of node 6. In this particular case $L = 2 \cdot 3 = 6$; $I = 2 \cdot 3 - 1 - 1 = 4$; $R \equiv L = 6$.

forces. When the program is run with the detailed print switch triggered (ISW = +1), the left and right cut forces are computed from the solution displacement vector and subsequently printed in condensed format (under the FORVEC header). Inspection of these results showed that corresponding left and right cut internal nodal forces differed by the proper amount, $\mu^* = 25.455^\circ$.

CONCLUDING REMARKS

The DMAP sequence presented in APPENDIX A, permits the NASTRAN user to solve a class steady state dynamically loaded periodic structures, wherein the internal forces and resulting response at the periodic ends of the typical repeating substructure are related by a known complex phase relation, $e^{i\mu^*}$. The DMAP sequence is general and need not be changed from one problem to the next. When using the methodology presented here, one should be extremely careful that the CV100, CV010, CV001 partitioning vectors are prepared properly. For large problems, a preprocessor should be written which automatically generates these vectors. One should also be careful to allow for SPC, MPC and OMIT cards which compact the solution vector and consequently should be taken into account in the preparation of the partitioning vectors. The user is strongly advised to study the sample demonstration problem presented here before undertaking anymore complicated problems.

At this point, the DMAP sequence has been checked out for a set of small size problems, therefore comments regarding computer run time on large problems cannot be made at this time. Some of the DMAP operations can be increased in efficiency by employing the matrix operation ADD5 DMAP module in place of repeatedly employing the matrix ADD DMAP module. The ADD5 routine was not used in the 1108, level 15.5 version of NASTRAN due to the fact that the system did not consistently successfully add a string of 5 matrices during certain checkout phases of the programming.

Finally, it is advised that before attempting to exercise the DMAP sequence presented in APPENDIX A, one should run the demonstration problem as a benchmark check in. If a Univac 1108, level 15.5 version is used, it may be necessary to increase the "max-files" to 40 in NTRAN\$.

REFERENCES

1. Brillouin, L., "Wave Propagation in Periodic Structures", Dover Publications, Inc., New York, 1946.
2. Elachi, C., "Waves in Active and Passive Periodic Structures", Proceedings of the IEEE, Vol. 64, No. 12, Dec. 1976.
3. Heckl, M. A., "Investigations on the Vibrations of Grillages and Other Simple Beam Structures, Journal of the Acoustical Society of America, Vol. 36, 1964.

4. Abrahamson, A. L., "Flexural Wave Mechanics - an Analytical Approach to the Vibration of Periodic Structures Forced by Convected Pressure Fields", Journal of Sound and Vibration, Vol. 28, 1973.
5. Murakami, H. and Luco, E., "Seismic Response of a Periodic Array of Structures", Journal of the Engineering Mechanics Div., ASCE, Oct. 1977.
6. Mead, D. J., "A General Theory of Harmonic Wave Propagation in Linear Periodic Systems with Multiple Coupling", Journal of Sound and Vibration, Vol. 27, No. 2, Feb. 1973.
7. Orris, R. M. and Petyt, M., "A Finite Element Study of Harmonic Wave Propagation in Periodic Structures", Journal of Sound and Vibration, Vol. 33, No. (2), Feb. 1974.
8. Kalinowski, A. J. and Patel, J. S., "A Summary of NASTRAN Fluid/Structure Interaction Capabilities, NASTRAN Users' Experiences", Fifth Colloquium, NASA TM X-3428, Oct. 1976.

APPENDIX-A

(NASTRAN DEMONSTRATION PROBLEM INPUT)

N A S T R A N E X E C U T I V E C O N T R O L D E C K

ID NUSC PERIODIC STRUCTURE SAMPLE
 APP DISP
 SOL 8,n
 TIME 30
 DIAG 2,3,8,14,15
 DIAG 22
 ALTER 138

\$ DMPA INSTRUCTIONS FOR PERIODIC STRUCTURES (CODED BY A.J.KALINOWSKI)
 \$ ISW=+1 PRINT ... =-1 NO PRINT OF ALL KEY MATRICES FOR PERIODIC STR.
 PARAM //C,N,NOP/V,N,ISW=+1 \$
 PARAM //C,N,NOP/V,N,IMI=-1 \$
 PARAM //C,N,NOP/V,N,PURSW1=-1 \$
 \$ DEFINE ROW PARTITIONING VECTORS WITH DUMMY ADD OPERATION
 \$ WHERE CV100 CV010 CV001 ARE READ IN ON DMT BULK DATA
 ADD CV100,/RV100 \$
 ADD CV010,/RV010 \$
 ADD CV001,/RV001 \$
 COND MAR,ISW \$
 MATPRN RV100,RV010,RV001, ,// \$
 MATPRN CV100,CV010,CV001, ,// \$
 LABEL MAR \$
 \$ CONDITIONAL PRINT OF KDD,MDD, BDD BEFORE PARTITION APPLIED (
 COND KAL,ISW \$
 MATPRN KDD,MDD,BDD, ,// \$
 \$ SAVE ORIGINAL KDD MDD BDD MATRICES FOR PROCESSING FORCES AT CUTS
 ADD KDD,/SAVKDD \$
 ADD MDD,/SAVMDD \$
 ADD BDD,/SAVBDD \$
 LABEL KAL \$
 \$ PARTITION K,M,B MATRICES
 \$ PARTITION LL BLOCK
 PARTN KDD,CV100,RV100/ , , ,DKLL/C,N,1 \$
 PARTN MDD,CV100,RV100/ , , ,DMLL/C,N,1 \$
 PARTN BDD,CV100,RV100/ , , ,DBLL/C,N,1 \$
 \$ PARTITION LI BLOCK
 PARTN KDD,CV010,RV100/ , , ,DKLI/C,N,1 \$
 PARTN MDD,CV010,RV100/ , , ,DMLI/C,N,1 \$
 PARTN BDD,CV010,RV100/ , , ,DBLI/C,N,1 \$
 \$ PARTITION LR BLOCK
 PARTN KDD,CV001,RV100/ , , ,DKLR/C,N,1 \$
 PARTN MDD,CV001,RV100/ , , ,DMLR/C,N,1 \$
 PARTN BDD,CV001,RV100/ , , ,DBLR/C,N,1 \$
 \$ PARTITION IL BLOCK
 PARTN BDD,CV100,RV010/ , , ,DBIL/C,N,1 \$

PARTN KDD, CV100, RV010/,,, DKIL/C, N, 1 \$

PARTN MDD, CV100, RV010/,,, DMIL/C, N, 1 \$

\$ PARTITION II BLOCK

PARTN KDD, CV010, RV010/,,, DKII/C, N, 1 \$

PARTN MDD, CV010, RV010/,,, DMII/C, N, 1 \$

PARTN BDD, CV010, RV010/,,, DBII/C, N, 1 \$

\$ PARTITION IR BLOCK

PARTN KDD, CV001, RV010/,,, DKIR/C, N, 1 \$

PARTN MDD, CV001, RV010/,,, DMIR/C, N, 1 \$

PARTN BDD, CV001, RV010/,,, DBIR/C, N, 1 \$

\$ PARTITION RL BLOCK

PARTN KDD, CV100, RV001/,,, DKRL/C, N, 1 \$

PARTN MDD, CV100, RV001/,,, DMRL/C, N, 1 \$

PARTN BDD, CV100, RV001/,,, DBRL/C, N, 1 \$

\$ PARTITION RI BLOCK

PARTN KDD, CV010, RV001/,,, DKRI/C, N, 1 \$

PARTN MDD, CV010, RV001/,,, DMRI/C, N, 1 \$

PARTN BDD, CV010, RV001/,,, DBRI/C, N, 1 \$

\$ PARTITION RR BLOCK

PARTN KDD, CV001, RV001/,,, DKRR/C, N, 1 \$

PARTN MDD, CV001, RV001/,,, DMRR/C, N, 1 \$

PARTN BDD, CV001, RV001/,,, DBRR/C, N, 1 \$

\$CONDITIONAL PRINT OF PARTITIONS

COND KALIN, ISW \$

MATPRN DKLL, DMLL, DBLL, , , // \$

MATPRN DKLI, DMLI, DBLI, , , // \$

MATPRN DKLR, DMLR, DBLR, , , // \$

MATPRN DKIL, DMIL, DBIL, , , // \$

MATPRN DKII, DMII, DBII, , , // \$

MATPRN DKIR, DMIR, DBIR, , , // \$

MATPRN DKRL, DMRL, DBRL, , , // \$

MATPRN DKRI, DMRI, DBRI, , , // \$

MATPRN DKRR, DMRR, DBRR, , , // \$

LABEL KALIN \$

\$ *

\$ FORM PARTITIONS OF ASSEMBLED MATRIX MDDX, BDDX, KDDX

\$ *

\$ FORM LL BLOCK

\$

\$ FORM AMLL

ADD DMLL, DMLR/D1AMLL/V, Y, PONE/V, Y, CMST \$

ADD D1AMLL, DMRL/D2AMLL/V, Y, PONE/V, Y, CMST \$

ADD D2AMLL, DMRR/AMLL/V, Y, PONE/V, Y, PONE \$

PURGE KDD, MDD, BDD/PURSW1 \$

PURGE D1AMLL, D2AMLL/PURSW1 \$

\$ FORM ABLL
 ADD DBLL,DBLR/D1BLL/V,Y,PONE/V,Y,CMST \$
 ADD D1BLL,DMLR/D2BLL/V,Y,PONE/V,Y,NSMSTO \$
 ADD D2BLL,DKLR/D3BLL/V,Y,PONE/V,Y,SMSBO \$
 ADD D3BLL,DBRR/D4BLL/V,Y,PONE/V,Y,PONE \$
 PURGE D1ABLL,D2ABLL,D3ABLL/PURSW1 \$
 ADD D4BLL,DMRL/D5BLL/V,Y,PONE/V,Y,SMSTO \$
 ADD D5BLL,DKRL/ABLL/V,Y,PONE/V,Y,NSMSBO \$
 PURGE D4BLL,D5BLL/PURSW1 \$
 \$ FORM AKLL
 ADD DKLL,DKLR/D1KLL/V,Y,PONE/V,Y,CMST \$
 ADD D1KLL,DBLR/D2KLL/V,Y,PONE/V,Y,NSMSTO \$
 ADD D2KLL,DKRL/D3KLL/V,Y,PONE/V,Y,CMST \$
 ADD D3KLL,DKRR/D4KLL/V,Y,PONE/V,Y,PONE \$
 ADD D4KLL,DBRL/AKLL/V,Y,PONE/V,Y,SMSTO \$
 PURGE D1KLL,D2KLL,D3KLL,D4KLL/PURSW1 \$
 \$ FORM LI BLOCK
 \$
 \$ FORM AMLI
 ADD DMLI,DMRI/AMLI/V,Y,PONE/V,Y,CMST \$
 \$ FORM ABLI
 ADD DBLI,DBRI/D1BLI/V,Y,PONE/V,Y,CMST \$
 ADD D1BLI,DMRI/D2BLI/V,Y,PONE/V,Y,SMSTO \$
 ADD D2BLI,DKRI/ABLI/V,Y,PONE/V,Y,NSMSBO \$
 PURGE D1BLI,D2BLI/PURSW1 \$
 \$ FORM AKLI
 ADD DKLI,DKRI/D1KLI/V,Y,PONE/V,Y,CMST \$
 ADD D1KLI,DBRI/AKLI/V,Y,PONE/V,Y,SMSTO \$
 PURGE D1KLI/PURSW1 \$
 \$ FORM IL BLOCK
 \$
 \$ FORM AMIL
 ADD DMIL,DMIR/AMIL/V,Y,PONE/V,Y,CMST \$
 \$ FORM ABIL
 ADD DBIL,DBIR/D1BIL/V,Y,PONE/V,Y,CMST \$
 ADD D1BIL,DMIR/D2BIL/V,Y,PONE/V,Y,NSMSTO \$
 ADD D2BIL,DKIR/ABIL/V,Y,PONE/V,Y,SMSBO \$
 PURGE D1BIL,D2BIL/PURSW1 \$
 \$ FORM AKIL
 ADD DKIL,DKIR/D1KIL/V,Y,PONE/V,Y,CMST \$
 ADD D1KIL,DBIR/AKIL/V,Y,PONE/V,Y,NSMSTO \$
 PURGE D1KIL/PURSW1 \$
 \$ FORM II BLOCK
 \$ AMII SAME AS DMII ABII SAME AS DMII AKII SAME AS DKII
 \$ FORM RL BLOCK

```

ADD UMATR,/ABRL/V,Y,SMSBO $
ADD UMATR,/AKRL/V,Y,CMST $
$ FORM RR BLOCK
ADD UMATR,/AKRR/V,Y,NONE $
$ THE LR,IR,RI BLOCKS ARE NULL
$ PRINT BLOCKS BEFORE ASSEMBLY
COND DEB,ISW $
MATPRN AMLL,ABLL,AKLL,/// $
MATPRN AMLI,ABLI,AKLI,/// $
MATPRN AMIL,ABIL,AKIL,/// $
MATPRN ABRL,AKRL,AKRR,/// $
PRTPARM //C,N,0$
LABEL DEB$
$ *
$ NEXT ASSEMBLE BLOCKS WITH MERGE
$ *
$ MERGE LL BLOCK
MERGE LIXLI,,,AKLL,CV100,RV100/KDDXLL/C,N,1 $
MERGE LIXLI,,,AMLL,CV100,RV100/MDDXLL/C,N,1 $
MERGE LIXLI,,,ABLL,CV100,RV100/BDDXLL/C,N,1 $
$ MERGE LI BLOCK
MERGE LIXL2,,,AKLI,CV010,RV100/KDDXLI/C,N,1 $
MERGE LIXL2,,,AMLI,CV010,RV100/MDDXLI/C,N,1 $
MERGE LIXL2,,,ABLI,CV010,RV100/BDDXLI/C,N,1 $
$ FORM PARTIAL SUM
ADD KDDXLL,KDDXLI/SUMK1 $
ADD MDDXLL,MDDXLI/SUMM1 $
ADD BDDXLL,BDDXLI/SUMB1 $
$ PURGE COMPONENTS OF PARTIAL SUM NOT NEEDED ANY MORE
PURGE KDDXLL,KDDXLI,MDDXLL,MDDXLI,BDDXLL,BDDXLI/PURSW1 $
$ MERGE IL BLOCK
MERGE L2XLI,,,AKIL,CV100,RV010/KDDXIL/C,N,1 $
MERGE L2XLI,,,AMIL,CV100,RV010/MDDXIL/C,N,1 $
MERGE L2XLI,,,ABIL,CV100,RV010/BDDXIL/C,N,1 $
$ CONTINUE PARTIAL SUM
ADD SUMK1,KDDXIL/SUMK2 $
ADD SUMM1,MDDXIL/SUMM2 $
ADD SUMB1,BDDXIL/SUMB2 $
COND JOHN,ISW $
MATPRN SUMK1,KDDXIL,SUMK2,SUMM1,MDDXIL// $
MATPRN SUMM2,SUMB1,BDDXIL,SUMB2,/$
LABEL JOHN $
$ PURGE COMPONENTS OF PARTIAL SUM NOT NEEDED ANY MORE
PURGE SUMK1,KDDXIL,SUMM1,MDDXIL,SUMB1,BDDXIL/PURSW1 $
$ MERGE II BLOCK

```

```

MERGE L2XL2,,,DKII,CV010,RV010/KDDXII/C,N,1 $
MERGE L2XL2,,,DMII,CV010,RV010/MDDXII/C,N,1 $
MERGE L2XL2,,,DBII,CV010,RV010/BDDXII/C,N,1 $
$ CONTINUE PARTIAL SUM
ADD SUMK2,KDDXII/SUMK3 $
ADD SUMM2,MDDXII/MDDX $
$ WHERE MDDX IS THE FINAL MASS MATRIX SUM
ADD SUMB2,BDDXII/SUMB3 $
COND BULL,ISW $
MATPRN SUMK2,KDDXII,SUMK3,SUMM2,MDDXII// $
MATPRN MDDX,SUMB2,BDDXII,SUMB3,//$
LABEL BULL$
$ PURGE COMPONENTS OF PARTIAL SUM NOT NEEDED ANY MORE
PURGE SUMK2,KDDXII,SUMM2,MDDXII,SUMB2,BDDXII/PURSW1 $
$ MERGE RL BLOCK
MERGE LIXLI,,,AKRL,CV100,RV001/KDDXRL/C,N,1 $
MERGE LIXLI,,,ABRL,CV100,RV001/BDDXRL/C,N,1 $
$ CONTINUE PARTIAL SUM
ADD SUMK3,KDDXRL/SUMK4 $
ADD SUMB3,BDDXRL/BDDX $
$ WHERE BDDX IS THE FINAL MATRIX SUM
COND PILL,ISW $
MATPRN SUMK3,KDDXRL,SUMK4,SUMB3,BDDXRL// $
MATPRN BDDX,,,,//$
LABEL PILL$
$ PURGE COMPONENTS OF PARTIAL SUM NOT NEEDED ANY MORE
PURGE SUMK3,KDDXRL,SUMB3,BDDXRL/PURSW1 $
$ MERGE RR BLOCK
MERGE LIXLI,,,AKRR,CV001,RV001/KDDXRR/C,N,1 $
$ CONTINUE PARTIAL SUM
ADD SUMK4,KDDXRR/KDDX $
$ WHERE KDDX IS THE FINAL SUMMED MATRIX
COND BOOK,ISW $
MATPRN SUMK4,KDDXRR,KDDX,//$
LABEL BOOK $
$ PURGE COMPONENTS OF PARTIAL SUM NOT NEEDED ANY MORE
PURGE SUMK4,KDDXRR/PURSW1 $
$ *
$ *** NOW ALL THE KDDX BDDX AND MDDX MATRICES ARE FORMED
$ *
COND JACK,ISW $
MATPRN MDDX,BDDX,KDDX,//$
LABEL JACK$
ALTER 139,139
FRRD CASEXX,USETD,DLT,FRL,GMD,GOD,KDDX,BDDX,MDDX,,DIT/UDVF,PSF,PDF,PPF/

```

C,N,DISP/C,N,DIRECT/V,N,LUSETD/V,N,MPCF1/V,N,SINGLE/V,N,OMIT/
V,N,NONCUP/V,N,FRQSET/C,Y,DECOMPT=1 \$

ALTER 140

COND ABE,ISW \$

\$ PRINT THE FORCE VECTORS USED BY THE EQUIVALENT PERIODIC STRUCTURE

MATPRN PDF,PSF,PPF,.,// \$

\$ PROCESS THE LEFT AND RIGHT PERIODIC CUT FORCES

ADD SAVMDC,SAVKDD/DSAV/V,Y,NOMEG2/V,Y,PONE \$

ADD DSAV,SAVBDD/KNET/V,Y,PONE/V,Y,FIOMFG \$

PURGE DSAV/PURSW1 \$

MPYAD KNET,UDVF,/FORVEC/C,N,0/C,N,1/C,N,0/C,N,1 \$

MATPRN KNET,UDVF,FORVEC,.,// \$

LABEL ABE \$

ENDALTER

CEND

C A S E C O N T R O L D E C K E C H O

TITLE = PERIODIC STRUCTURE (FIRST SAMPLE)

MAXLINES = 30000

DLOAD = 10

FREQUENCY = 1

OLOAD = ALL

STRESS = ALL

DISPLACEMENT = ALL

BEGIN BULK

SORTED BULK DATA ECHO

	1	2	3	4	5	6	7	8	9	10
CDAMP2	101	4.07293	1	2						
CDAMP2	106	8.14587	6	2						
CDAMP2	107	4.07293	7	2						
CQDMEM	1	1	2	5	4	3				
CQDMEM	2	1	1	6	5	2				
CQDMEM	3	1	4	5	8	9				
CQDMEM	4	1	5	6	7	8				
DAREA	21	3	2	-49.8972						
DAREA	21	4	2	-99.7944						
DAREA	210	3	2	-49.9742						
DLOAD	10	1.	1.	100	1.	101				
DMI	CV001	0	2	1	1	18	1			
DMI	CV001	1	13	1.	1.	1.	1.	1.		D0G5
+OGS	1.									
DMI	CV010	0	2	1	1	18	1			
DMI	CV010	1	7	1.	1.	1.	1.	1.		P1G5
+IGS	1.									
DMI	CV100	0	2	1	1	18	1			
DMI	CV100	1	1	1.	1.	1.	1.	1.		CAT5
+ATS	1.									
DMI	LIXLI	0	2	1	1	12	12			
DMI	LIXLI	1	1	.0						
DMI	LIXL2	0	2	1	1	12	12			
DMI	LIXL2	1	1	.0						
DMI	L2XLI	0	2	1	1	12	12			
DMI	L2XLI	1	1	.0						
DMI	L2XL2	0	2	1	1	12	12			
DMI	L2XL2	1	1	.0						
DMI	UMATR	0	6	1	2	6	6			
DMI	UMATR	1	1	1.						
DMI	UMATR	2	2	1.						
DMI	UMATR	3	3	1.						
DMI	UMATR	4	4	1.						
DMI	UMATR	5	5	1.						
DMI	UMATR	6	6	1.						
DPHASE	23	3	2	28.6378						
DPHASE	23	4	2	38.18377						
DPHASE	230	3	2	22.27387						
FREQ	1	3000.								
GRDSET						3456				
GRID	1		.0	.0	.0					
GRID	2		.0	1.0	.0					
GRID	3		.0	2.0	.0					
GRID	4		1.0	2.0	.0					
GRID	5		1.0	1.0	.0					
GRID	6		1.0	.0	.0					
GRID	7		2.0	.0	.0					
GRID	8		2.0	1.0	.0					
GRID	9		2.0	2.0	.0					
MAT2	10	345600.	345600.	.0	345600.			.000096		
PARAM	CMST	.9029168	.0							
PARAM	FIOMEG	1.0-20	18849.55							
PARAM	NOMEG2	-3.553	+8.0							
PARAM	NONE	-1.0	.0							
PARAM	NSMSBO	-2.280	-5.0							
PARAM	NSMSTO	-8108.830	.0							
PARAM	PONE	+1.0	.0							
PARAM	SMSBO	+2.280	-5.0							
PARAM	SMSTO	+8108.830	.0							
PQDMEM	1	10	1.0							
RLOAD1	100	21		23	22					
RLOAD1	101	210		230	22					
TABLED1	22									PULS1
+ULS1	0.0	1.0	100000.	1.0	ENDT					
ENDDATA										

APPENDIX B (NASTRAN DEMONSTRATION PROBLEM OUTPUT)

FREQUENCY = 3.000000+03

COMPLEX LOAD VECTOR
(REAL/IMAGINARY)

POINT ID.	TYPE	T1	T2	T3	R1	R2	R3
3	G	.0	-9.003838+01	.0	.0	.0	.0
		.0	-4.285621+01	.0	.0	.0	.0
4	G	.0	-7.844159+01	.0	.0	.0	.0
		.0	-6.169147+01	.0	.0	.0	.0

FREQUENCY = 3.000000+03

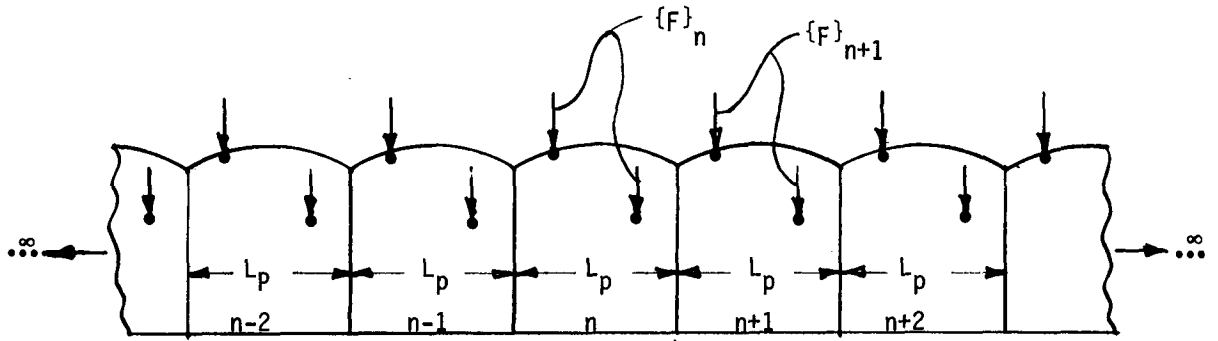
COMPLEX STRESSES IN QUADRILATERAL MEMBRANES (CODMEM)
(REAL/IMAGINARY)

ELEMENT ID.	- STRESSES IN ELEMENT COORDINATE SYSTEM -							
	real σ_{xx}	NORMAL σ_{yy}	real σ_{yy}	real σ_{xy}	NORMAL σ_{xx}	imag σ_{xx}	imag σ_{yy}	SHEAR σ_{xy}
1	-9.069812+01//	-9.069812+01	.0	//	-4.316528+01	-4.316528+01//	.0	
2	-9.808248+01//	-9.808248+01	.0	//	-2.207309+01	-2.207309+01//	.0	
3	-7.895863+01//	-7.895863+01	.0	//	-6.209007+01	-6.209007+01//	.0	
4	-9.080797+01//	-9.080797+01	.0	//	-4.314243+01	-4.314243+01//	.0	

TABLE B-1

NASTRAN-EXACT SOLUTION COMPARISON

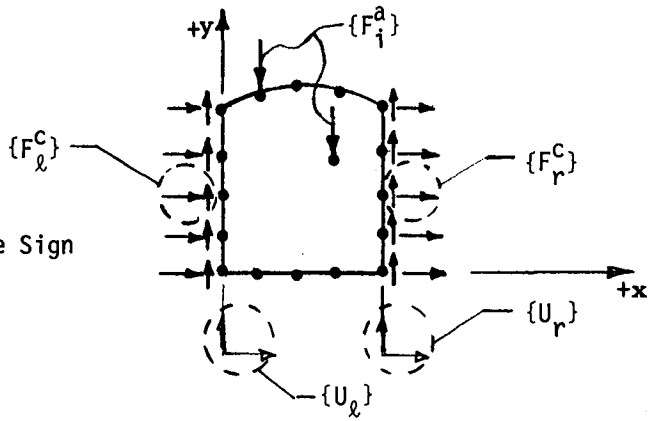
p element	NASTRAN p , psi	EXACT p , psi	NASTRAN Phase of p	EXACT Phase of p
1	100.53	100.00	12.683°	12.728°
2	100.44	100.00	25.451°	25.456°
3	100.44	100.00	38.180°	38.183°
4	100.53	100.00	25.412°	25.456°



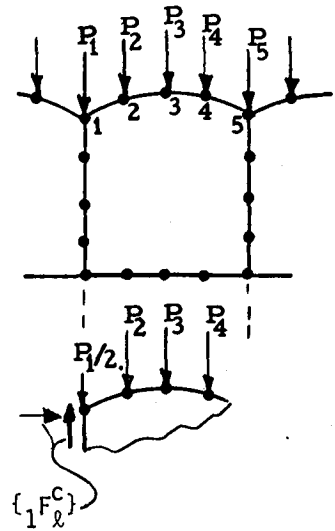
a) Total Periodic Structure

left cut right cut

b) n^{th} Substructure Sign Convention



c) Force Decomposition At Cut



$({}_1F_l^a)_y = P_1/2 \dots$ applied force at node on left cut
 $({}_2F_i^a)_y = P_2 \dots$ applied force at node off left cut

Fig. 1 Periodic Structure Notation

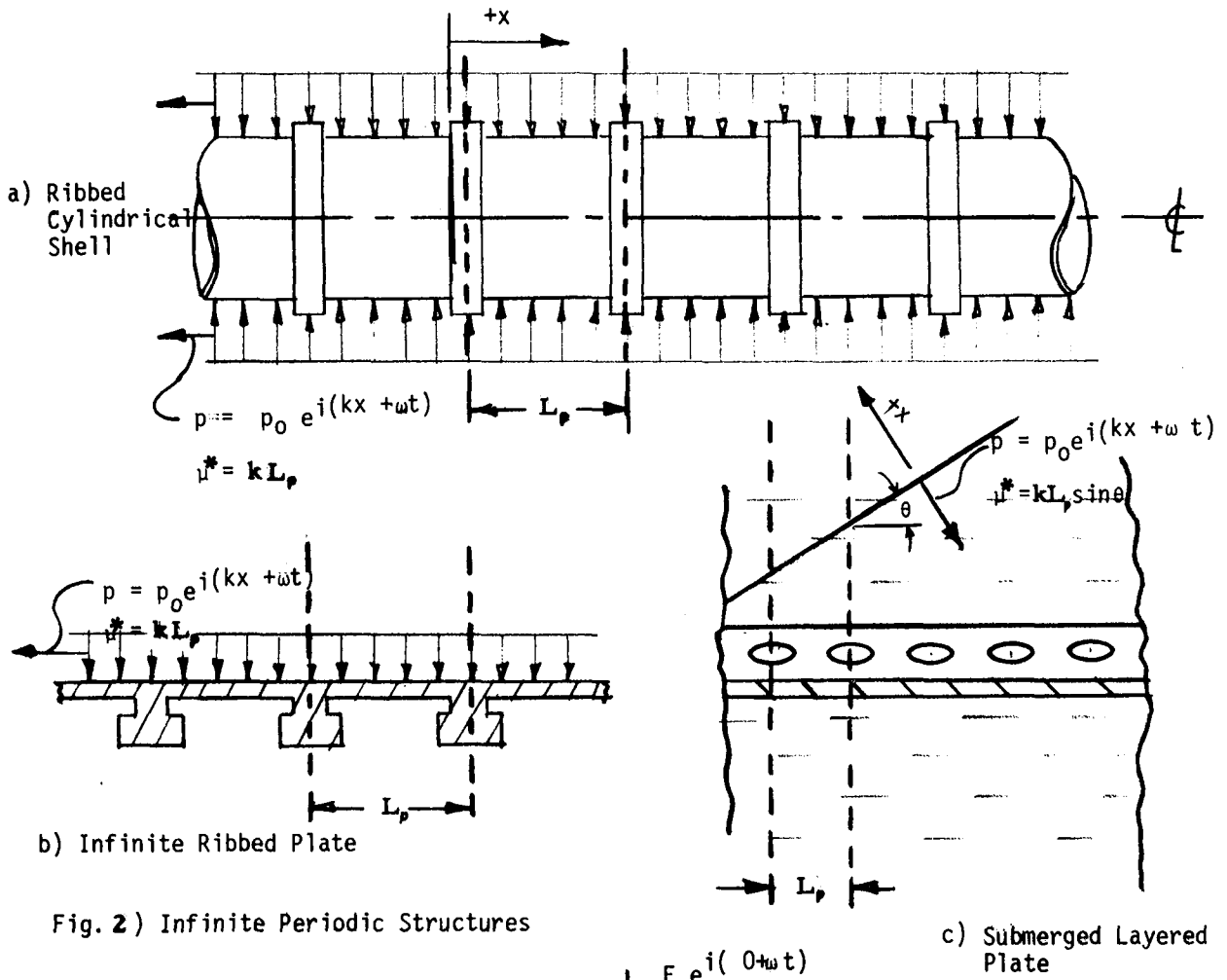


Fig. 2) Infinite Periodic Structures

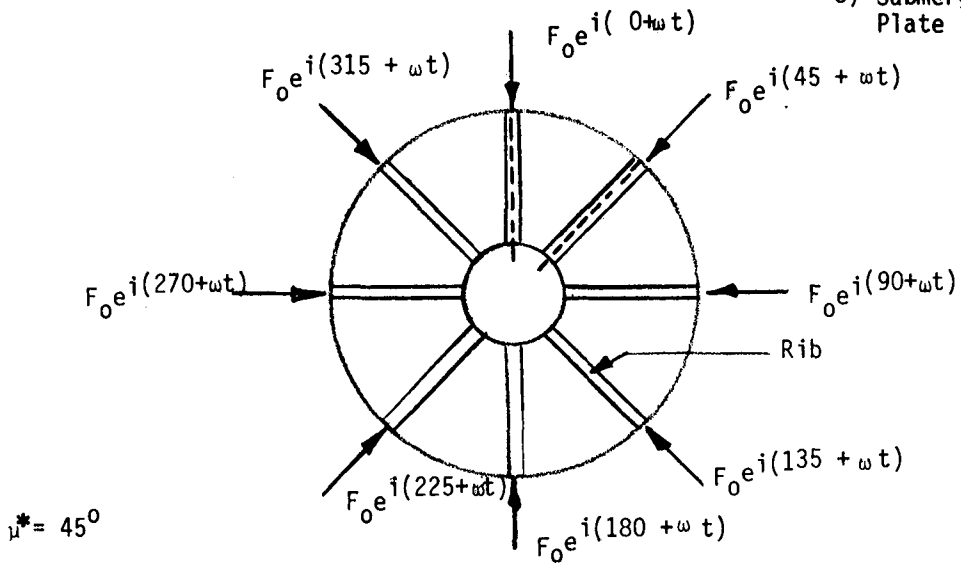


Fig. 3 Cyclic Periodic Structure

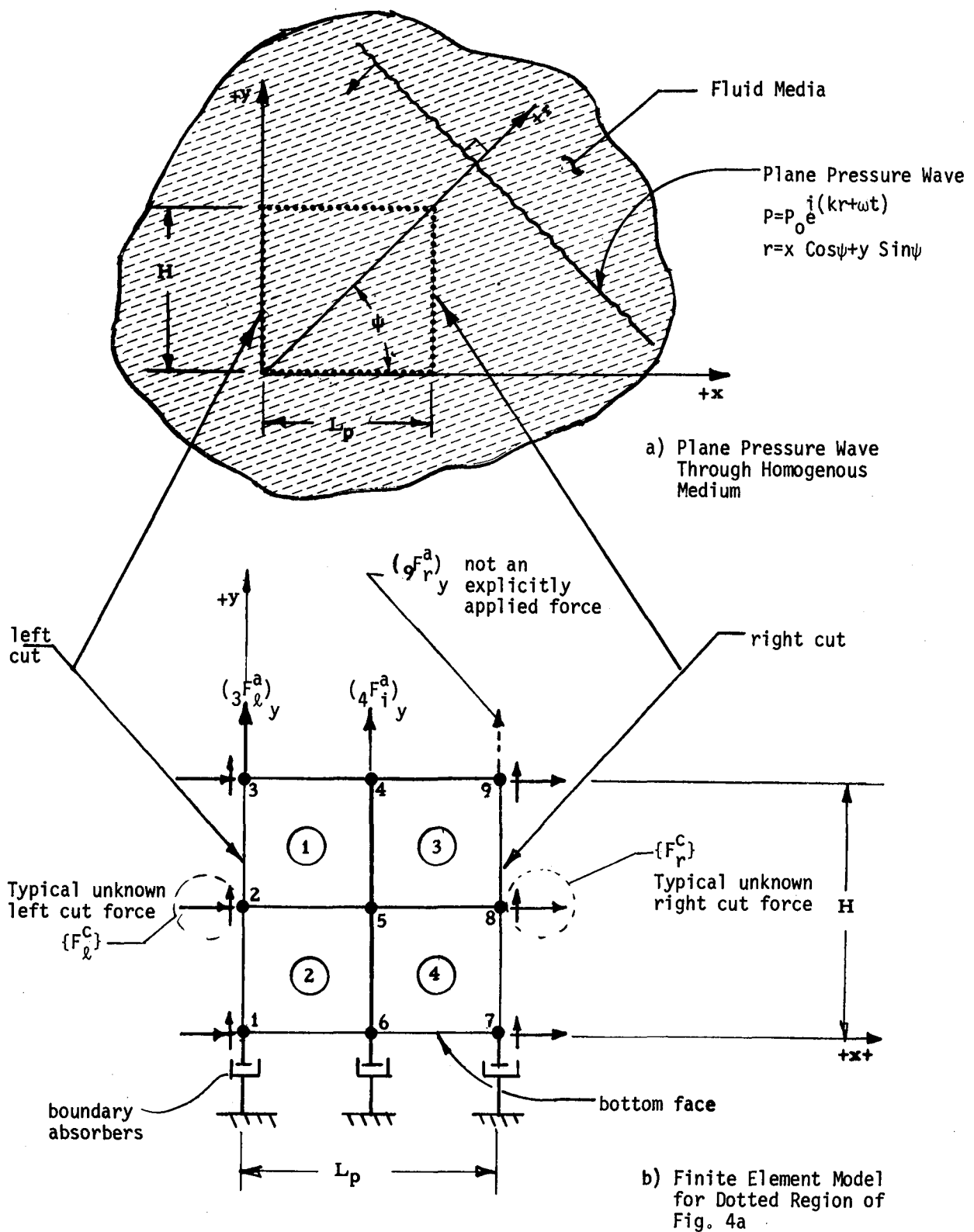


Fig. 4 Demonstration Problem